Prenyltransferase: Determination of the Binding Mechanism and Individual Kinetic Constants for Farnesylpyrophosphate Synthetase by Rapid Quench and Isotope Partitioning Experiments†

F. Mark Laskovics and C. Dale Poulter*

ABSTRACT: The 1′–4 condensation reaction catalyzed by farnesylpyrophosphate synthetase was examined by using rapid quench and isotope partitioning experiments. E·Mg^{2+}-isopentenyl-PP (PP = pyrophosphate) is not catalytically competent, as evidenced by failure to trap the complex with Mg^{2+}-geranyl-PP at concentrations as high as 3.2 mM. In contrast, the concentration of Mg^{2+}-isopentenyl-PP required for one-half maximal trapping ($K_{1/2}$) of E·Mg^{2+}-geranyl-PP is 1.4 μM. The results strongly support an ordered mechanism for the 1′–4 condensation reaction, with addition of the allylic substrate before Mg^{2+}-isopentenyl-PP. At short reaction times, a burst phase corresponding to accumulation of Mg^{2+}-farnesyl-PP on the surface of the enzyme, followed by a slower, steady-state release of products, is observed. Evaluation of individual kinetic constants for the reaction indicates that the rates for addition of Mg^{2+}-geranyl-PP to the enzyme (k_1 = 4.9 × 10^6 M^{-1} s^{-1}) and addition of Mg^{2+}-isopentenyl-PP to E·Mg^{2+}-geranyl-PP (k_3 = 2 × 10^6 M^{-1} s^{-1}) are below the diffusion-controlled limit. The rate-limiting step at steady state is isomerization of E·Mg^{2+}-farnesyl-PP·Mg^{2+}-PP_i or release of products (k_6 = 0.1 s^{-1}). During the course of isotope partitioning experiments with E·Mg^{2+}-geranyl-PP, a new dual isotope procedure was developed which minimizes difficulties encountered during workup. In addition, for enzymes such as farnesyl-PP synthetase that catalyze irreversible reactions, the dual isotope approach is both sensitive and extremely easy to execute.

Farnesylpyrophosphate synthetase (EC 2.5.1.1), a key prenyl transfer enzyme in the biosynthesis of cholesterol, dolichol, and perhaps ubiquinones, catalyzes the 1′–4 condensation (Poulter et al., 1977) of dimethylallyl-PP (PP = pyrophosphate)[1] and geranyl-PP with isopentenyl-PP (Scheme I). The enzyme has been purified to homogeneity from *Saccharomyces cerevisiae* (Eberhardt & Rilling, 1975), *Phycomyces blakeleeanus* (H. C. Rilling, unpublished results), avian liver (Reed & Rilling, 1975), and porcine liver (Yeh & Rilling, 1977; Barnard et al., 1978). All sources yield enzyme which is a dimer of approximately 84 000 daltons. The more extensively studied avian enzyme has two identical subunits (Reed & Rilling, 1975). Each has a single catalytic site with two well-defined regions. One, the isopentenyl region, only binds isopentenyl-PP, while the other, the allylic region, binds the allylic substrates dimethylallyl-PP and geranyl-PP, as well as isopentenyl-PP (Reed & Rilling, 1976; King & Rilling, 1977; Laskovics et al., 1979). In addition, a divalent metal, Mg^{2+} or Mn^{2+}, is required for catalysis. Kinetic and equilibrium binding studies indicate that the metal ions are incorporated as the monometal salts of the pyrophosphate esters, the true substrates for the enzyme.

Initial velocity measurements, including product inhibition patterns (Holloway & Popjak, 1967; Popjak et al., 1969), using a soluble enzyme preparation from porcine liver were interpreted in terms of an ordered sequential mechanism, with addition of geranyl-PP before isopentenyl-PP and release of farnesyl-PP before PP_i. We recently reported a kinetic study for farnesyl-PP synthetase from avian liver which included product inhibition and dead-end inhibition with fluorinated analogues of the substrates (Laskovics et al., 1979). The avian enzyme gave patterns typical of those expected for a random sequential mechanism. We pointed out, however, that the initial velocity patterns predicted for random and ordered addition of substrates are degenerate because isopentenyl-PP, analogues of isopentenyl-PP, and PP_i bind at both the homoallylic and allylic regions of the active site. In order to distinguish between the two possibilities, we undertook a series of rapid quench and isotope partitioning experiments. In addition to elucidation of the binding mechanism for farnesyl-PP synthetase, the individual kinetic constants for binding and release of substrates, catalysis, and a rate-limiting post-catalytic step were determined. Finally, a new procedure based on isotope ratios was developed for isotope partitioning experiments, which is especially useful in systems where isolation

Scheme I: 1′–4 Condensation Reactions Catalyzed by Farnesyl-PP Synthetase

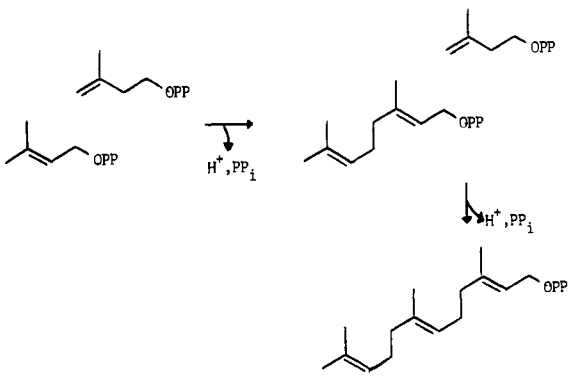

† From the Department of Chemistry, University of Utah, Salt Lake City, Utah 84112. *Received August 20, 1980.* This investigation was supported by Research Grants GM 21328 and RR 07092 from the National Institutes of Health. F.M.L. is a National Institutes of Health Postdoctoral Fellow (GM 06775). C.D.P. is an Alfred P. Sloan Fellow; Research Career Development Award from the National Institutes of Health, Grant HL 00084, 1975–1980.

[1] Abbreviations used: isopentenyl-PP, isopentenyl pyrophosphate; farnesyl-PP, farnesyl pyrophosphate; dimethylallyl-PP, dimethyallyl pyrophosphate; geranyl-PP, geranyl pyrophosphate; PP_i, inorganic pyrophosphate.

0006-2960/81/0420-1893$01.25/0

of the products in a quantitative and reproducible manner is difficult, or for enzymes that catalyze irreversible reactions.

Experimental Procedures

Materials

Enzymes. Crystalline avian liver farnesyl-PP synthetase (EC 2.5.1.1), specific activity 2 U/mg, was kindly provided by Professor H. C. Rilling. Calf mucosa alkaline phosphatase (EC 3.1.3.1), specific activity 1.1 U/mg, was purchased from Sigma and used without further purification.

Substrates. Geranyl-PP and isopentenyl-PP were prepared from the corresponding alcohols according to standard procedures (Cramer & Weiman, 1960; Donninger & Popjak, 1967; Cornforth & Popjak, 1969). The pyrophosphates were purified by ion-exchange chromatography on DEAE-Sephadex A-25 (Pharmacia) equilibrated with 0.05 M triethylammonium bicarbonate, pH 8.15, and developed with a linear gradient (0.05–0.65 M) of the same buffer. The purity of the organopyrophosphates was determined by TLC on phosphate-buffered silica gel H plates (E.M. Reagents) by using methanol/chloroform/water (10:10:3). Concentrations of stock solutions were determined by analysis for phosphate (Richards & Boyer, 1965).

Methods

Isotope Partitioning Experiments. (*a*) *Trapping of Enzyme·Mg^{2+}-[1-^{14}C]Isopentenyl-PP.* Two solutions (A and B) were prepared for each isotope partitioning experiment. Solution A contained the enzyme and a labeled substrate, while solution B contained unlabeled substrates. To look for trapping of E·Mg^{2+}-[1-^{14}C]isopentenyl-PP, solution A contained farnesyl-PP synthetase and [1-^{14}C]isopentenyl-PP (50 μCi/μmol) in 0.660 mL of 10 mM Pipes buffer, 10 mM magnesium chloride, 10 mM β-mercaptoethanol, and 0.25 μM potassium azide, pH 7.0. Solution B contained geranyl-PP and isopentenyl-PP in 0.400 mL of the above buffer, except the concentration of magnesium chloride was increased to 20 mM. Prior to mixing solutions A and B, 60 μL of A was withdrawn for a blank determination. The solutions were equilibrated at 4 °C before B was injected into rapidly stirred A. Samples (100 μL) were withdrawn at various times and injected into 100 μL of trifluoroacetic acid. The allylic pyrophosphates were decomposed to hydrocarbon-soluble material by heating the acid-quenched samples at 37 °C for 10 min. The resulting mixture was extracted with 1.0 mL of ligroine (90–120 °C), and radioactivity in 0.7 mL of the extract was determined by liquid scintillation spectrometry in 10 mL of 0.4% Omnifluor (New England Nuclear) in toluene.

(*b*) *Trapping of Enzyme·Mg^{2+}-[1-^{3}H]Geranyl-PP, Procedure 1.* The procedures described for isopentenyl-PP were followed through mixing of the two solutions, except that solution A contained enzyme and [1-^{3}H]geranyl-PP (69 μCi/μmol), while solution B contained geranyl-PP and [1-^{14}C]isopentenyl-PP. In this case, portions were quenched by addition to 100 μL of 100 mM lysine buffer, pH 12.5, followed by vigorous agitation with a vortex mixer and heat treatment at 80 °C for 1 min. A 75-μL portion of the lysine buffer was added to 0.35 mL of 0.3 M hydrochloric acid, and the resulting mixture was heated at 37 °C for 10 min to hydrolyze the allylic pyrophosphates. The solution was extracted as previously described, and synthesis of farnesyl-PP was determined by incorporation of radioactivity into acid-labile material.

The remainder of the quenched sample (125 μL) was diluted with 0.25 mL of deionized water and adjusted to pH 10.5 by addition of 4 M acetate buffer, pH 4.78. The pyrophosphates were hydrolyzed by incubation with 5 mg (1.1 U/mg) of alkaline phosphatase at 37 °C for 12 h. The mixture was saturated with powdered sodium chloride and extracted with 1.5 mL of pentane. The pentane extract was dried over anhydrous sodium sulfate and concentrated to approximately 50 μL under a stream of dry nitrogen. Geraniol and farnesol were added as carriers, and the alcohols were separated by reversed-phase thin-layer chromatography by using 55:45 acetone/water (farnesol, R_f 0.21; geraniol, R_f 0.63; isopentenol, R_f 0.70). The alcohols were visualized by light staining with iodide. After the stain disappeared, the area corresponding to farnesol was scraped into a scintillation vial containing 0.5 mL of methanol and 10 mL of 0.4% Omnifluor in toluene. The ^{3}H/^{14}C ratio was determined by liquid scintillation spectrometry.

(*c*) *Trapping of Enzyme·Mg^{2+}-[1-^{3}H]Geranyl-PP, Procedure 2.* A solution of farnesyl-PP synthetase and [1-^{3}H]-geranyl-PP (69 μCi/μmol) was prepared in 10 mM Pipes buffer, pH 7.0, with 10 mM β-mercaptoethanol and 20 mM magnesium chloride. The solution was cooled to 4 °C before injection with rapid mixing of 200 μL of a solution of [1-^{14}C]isopentenyl-PP in the Pipes buffer. After 2 min at 4 °C, the sample was incubated at 37 °C for 20 min to complete the reaction. A 200-μL portion of the reaction mixture was mixed with a solution containing 700 μL of 35 mM lysine buffer, pH 10.5, and 5 mg (1.1 U/mg) of alkaline phosphatase. The resulting mixture was incubated overnight, worked up, and chromatographed on the reversed-phase thin-layer system described in part b.

Observation of a Burst Phase. (a) A 0.10-mL portion of a solution at 4 °C containing 16 μg of farnesyl-PP synthetase (specific activity 0.32 U/mg) was injected into 1.9 mL of vigorously stirred 10 mM Pipes buffer, pH 7.0, 10 mM β-mercaptoethanol, 1 mM magnesium chloride, 4.5 μM [1-^{14}C]isopentenyl-PP (56 μCi/μmol), and 16 μM geranyl-PP also at 4 °C. Samples were removed at various times and assayed as described for the isotope partitioning experiments with [1-^{14}C]isopentenyl-PP (part a).

(b) Rapid quench experiments were carried out at 4 °C with a Durrum Multi-Mixer apparatus. Kinetic measurements were performed between 0.24 and 10.05 s by mixing equal volumes of enzyme (0.1 μM) and substrates (10 μM [1-^{14}C]isopentenyl-PP (56 μCi/μmol) and 36 μM geranyl-PP) in 10 mM Pipes buffer, pH 7.0, 10 mM β-mercaptoethanol, 1 mM magnesium chloride, and 0.1% BSA and quenching the mixture with an equal volume of 1.0 M potassium hydroxide. The product of the reaction, farnesyl-PP, has a much higher affinity for the plastic reaction lines than the more hydrophilic substrates, and the normal purge cycle did not adequately clear the lines of radioactivity. This problem was circumvented by repeatedly rinsing the lines with buffer between each run. The quenched samples were adjusted to pH 1 with 1.0 M hydrochloric acid and heated at 37 °C for 10 min. The procedures for workup and determination of radioactivity were identical with those described previously for [1-^{14}C]isopentenyl-PP (part a).

Theory

For two substrates, A and B, which contain different isotopes that can be counted in the presence of one another (i.e., ^{3}H and ^{14}C), the radioactivity of the product (A*–B*) as a function of time due to incorporation of isotope from A* in the isotope partitioning scheme (Scheme II) is given by eq 1, where S_1 is the specific activity of A* (μCi/μmol) in the pulse solution, S_2 is the specific activity of A* (μCi/μmol) after

Scheme II

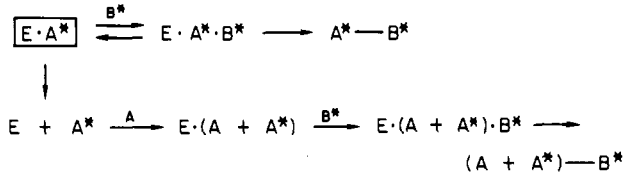

$$DPM_A^t = (2.2 \times 10^6 \text{ dpm}/\mu\text{Ci})[(S_1PE_{tot} + S_2(1 - P)E_{tot}) + (I_t - 1)S_2E_{tot}] \quad (1)$$

the chase solution is added, E_{tot} is the total number of moles of active sites, P represents the moles of E·A* which are trapped and is expressed as a mole fraction of E_{tot}, and I_t is the number of catalytic cycles at time t. The first two terms in eq 1 represent the radioactivity incorporated into product from A* and (A* + A), respectively, during the first turnover of the enzyme, and the third term denotes the radioactivity incorporated into the product from subsequent turnovers. Upon rearrangement, eq 1 becomes

$$DPM_A^t = (2.2 \times 10^6 \text{ dpm}/\mu\text{Ci})[(S_1 - S_2)P + I_tS_2]E_{tot} \quad (2)$$

The rate of incorporation of radioactivity from B* into product is given by eq 3, where S is the specific activity of B*

$$DPM_B^t = (2.2 \times 10^6 \text{ dpm}/\mu\text{Ci})(S_3I_tE_{tot}) \quad (3)$$

(μCi/μmol) after the chase solution is added.

The isotope ratio in A*–B* can be indexed to the number of times the enzyme has turned over by eq 4. I_t can be

$$\frac{DPM_A^t}{DPM_B^t} = \frac{(S_1 - S_2)P}{S_3I_t} + \frac{S_2}{S_3} \quad (4)$$

determined experimentally by adjusting concentrations so that [B] < [A] and by measuring the fraction of B*, f_t, incorporated into A*–B* as a function of time, t, where

$$f_t = \frac{DPM_B^t \text{ in A*–B*}}{DPM_B^\infty \text{ in A*–B*}} \quad (5)$$

Since B is the limiting substrate, N, the minimum number of turnovers required to approach equilibrium or the number of turnovers at $t = \infty$ for enzymes that catalyze irreversible reactions, is given by

$$N = \frac{[A^*–B^*]}{[E_t]} \quad (6)$$

and

$$I_t = Nf_t \quad (7)$$

Thus, eq 4 becomes

$$DPM_A^t/DPM_B^t = \left(\frac{(S_1 - S_2)P}{S_3N}\right)\frac{1}{f_t} + \frac{S_2}{S_3} \quad (8)$$

and a plot of DPM_A/DPM_B vs. the reciprocal of f_t should be linear with a slope proportional to P, the mole fraction of E_{tot} trapped in the first turnover.

Since the concentration of A in the chase is normally much greater than the concentration of A* in the pulse, $S_1 \gg S_2$, and $S_1 - S_2 \approx S_1$. Thus, eq 8 becomes

$$\frac{DPM_A^t}{DPM_B^t} = \left(\frac{S_1P}{S_3N}\right)\frac{1}{f_t} + \frac{S_2}{S_3} \quad (9)$$

T, the mole fraction of E·A* trapped upon addition of the chase, is determined from P as shown in eq 10, where E·A^*

$$T = P\left(\frac{E_{tot}}{E \cdot A^*}\right) \quad (10)$$

is calculated from the dissociation constant for A and from the concentrations of enzyme and A* in the pulse. Evaluation of T from plots of DPM_A^t/DPM_B^t vs. $1/f_t$ is the method of choice when $K_{1/2}$, the concentration of B* required to trap half of E·A*, is 10–100 μM or greater. However, for enzymes with low values for $K_{1/2}$, it is often inconvenient to determine DPM_A^t/DPM_B^t at low conversions where the isotope ratios are changing rapidly and the method is most sensitive.

Another approach, suitable when $K_{1/2}$ is small, is available for enzymes that catalyze reactions irreversibly or for enzymes where the catalytic step can be rendered irreversible by the appropriate coupling reaction. In such cases at $t = \infty$, f_t = 1 and eq 9 becomes

$$\frac{DPM_A^\infty}{DPM_B^\infty} = \frac{S_1P}{S_3N} + \frac{S_2}{S_3} \quad (11)$$

By the appropriate adjustment of specific activities where $S_2 \ll S_3$, eq 11 reduces to

$$\frac{DPM_A^\infty}{DPM_B^\infty} = \frac{S_1P}{S_3N} \quad (12)$$

and T can again be evaluated from P according to eq 10.

Scheme III: Isotope Partitioning

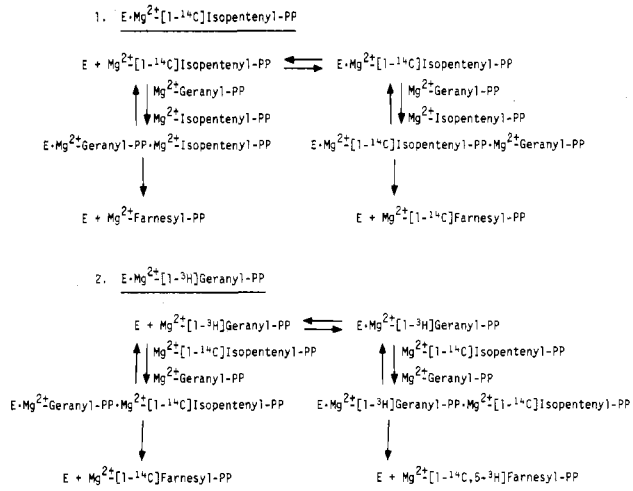

Results

Isotope Partitioning with Enzyme·Mg^{2+}-[1-^{14}C]Isopentenyl-PP. The design of the isotope partitioning experiments is presented in Scheme III. Part 1 in the scheme represents experiments for trapping E·Mg^{2+}-[1-^{14}C]isopentenyl-PP by chasing the complex with a solution containing a large excess of unlabeled Mg^{2+}-isopentenyl-PP and Mg^{2+}-geranyl-PP. The range of concentrations used in five separate runs are listed in Table I, and typical plots are shown in Figure 1. Individual points are the average of duplicate determinations. In each case, the initial rate for formation of Mg^{2+}-[1-^{14}C]farnesyl-PP is linear, and the y intercepts were determined by a least-squares analysis.

Farnesyl-PP synthetase does not bind Mg^{2+}-isopentenyl-PP regiospecifically to the homoallylic region of the active site, and formation of E·Mg^{2+}-isopentenyl-PP is always accompanied by E·(Mg^{2+}-isopentenyl-PP)$_2$. In principle, trapping could occur from the binary complex, the ternary complex, or both.

Table I: Isotope Partitioning Experiments with [1-^{14}C]Isopentenyl-PP

	before chase				after chase				
								trap	
run	enzyme (μM)	Mg^{2+}-[1-^{14}C]isopentenyl-PP[a] (μM)	E·Mg^{2+}-[1-^{14}C]isopentenyl-PP[b] (μM)	E·(Mg^{2+}-[1-^{14}C]isopentenyl-PP)$_2$[c] (μM)	Mg^{2+}-[1-^{14}C]isopentenyl-PP[d] (μM)	Mg^{2+}-isopentenyl-PP[d] (mM)	Mg^{2+}-geranyl-PP[d] (mM)	exptl[e]	100%[f]
1	0.228	13.8	0.017	0.188	8.3	1.5	3.2	−13 ± 9	135
2	0.15	6.8	0.019	0.103	4.1	1.0	2.15	−16 ± 7	151
3	0.15	4.1	0.025	0.082	2.5	1.0	2.15	−7 ± 8	198
4	0.15	1.4	0.031	0.035	0.8	1.0	2.15	20 ± 34	246
5	1.4	1.4	0.285	0.319	0.8	1.0	2.15	11 ± 6	2261

[a] Specific activity 56 μCi/μmol. [b] On the basis of a single binary complex, K_{diss} = 2.5 μM. [c] Calculated for K_{diss} = 2.5 μM. [d] Concentrations at t = 0. [e] y intercept of cpm vs. time plots; error limits are standard deviations from a least-squares analysis. [f] Expected value for 100% trap assuming only E·Mg^{2+}-[1-^{14}C]isopentenyl-PP is trapped and that Mg^{2+}-isopentenyl-PP is in the homoallylic region of the active site.

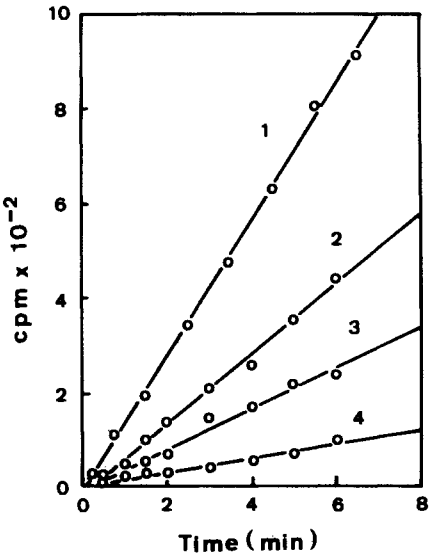

FIGURE 1: Isotope partitioning experiments with E·Mg^{2+}-[1-^{14}C]-isopentenyl-PP. The conditions for runs 1–4 are listed in Table I.

When the concentrations were adjusted appropriately, the ratio of binary complex to ternary complex was varied from 0.08 (run 1) to 0.89 (run 4). In each instance, however, the y intercepts of the initial velocity measurements were, within experimental error, zero, and the absence of a pulse as evidenced by a nonzero intercept (Caperelli et al., 1978) indicates that neither complex is trapped at concentrations of Mg^{2+}-geranyl-PP as high as 3.2 mM. The calculated y intercepts for 100% trap are conservative estimates since they represent the number of counts expected for trapping of the binary complex only. Interception of a catalytically competent form of E·Mg^{2+}-isopentenyl-PP generated by dissociation of E·(Mg^{2+}-isopentenyl-PP)$_2$ would give 100% values ranging from 278 cpm (run 4) to 2530 cpm (run 5) in addition to those listed in Table I.

Isotope Partitioning with Enzyme·Mg^{2+}-[1-^{3}H]Geranyl-PP. The design of experiments for trapping E·Mg^{2+}-[1-^{3}H]geranyl-PP is illustrated in part 2 of Scheme III. The straightforward acid-lability assay for determining the rate of synthesis of farnesyl-PP can no longer be used because the labeled substrate is also acid labile. A protocol designed specifically for [1-^{3}H]geranyl-PP which circumvents analytical problems associated with loss of material in a multistep workup that includes a chromatographic step is presented in Scheme IV. A solution containing Mg^{2+}, [1-^{3}H]geranyl-PP, and enzyme was equilibrated at 4 °C prior to addition of a chase containing Mg^{2+}, a large excess of [1-^{14}C]isopentenyl-PP, and unlabeled geranyl-PP. Samples taken at preselected times were quenched with hot base and divided into two portions. One portion was

Scheme IV: Protocol for Isotope Partitioning Experiments with E·Mg^{2+}-[1-^{3}H]Geranyl-PP

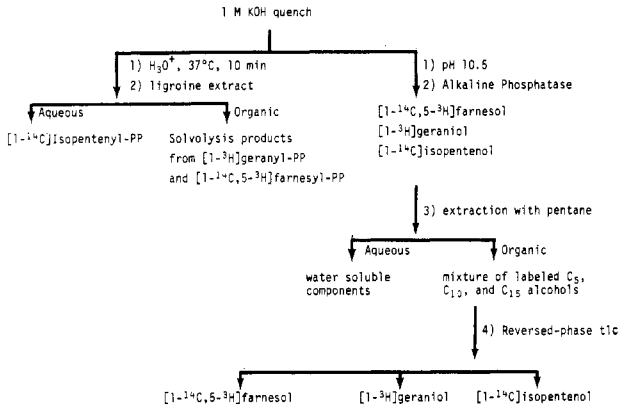

subjected to the standard acid-lability workup, and determination of the hydrocarbon-soluble ^{14}C counts gave a direct measure of the amount of [1-^{14}C,5-^{3}H]farnesyl-PP in the sample. The second portion was adjusted to pH 10.5 and treated with alkaline phosphatase. This procedure cleanly removes the pyrophosphates moiety from the substrates and product (Poulter & Rilling, 1976), giving a mixture of the corresponding C_5, C_{10}, and C_{15} alcohols. Carriers were added, and the three radioactive components were isolated by reversed-phase thin-layer chromatography under conditions which completely separate [1-^{14}C,5-^{3}H]farnesol from the other two alcohols. The ^{3}H/^{14}C ratio in farnesol was determined by standard procedures.

The data were analyzed by eq 13 (see Theory for a derivation) where S_1 is the specific activity of [1-^{3}H]geranyl-PP in the pulse solution, S_2 is the specific activity of [1-^{3}H]geranyl-PP after dilution with unlabeled substrate, S_3 is the specific activity of [1-^{14}C]isopentenyl-PP in the chase, P represents the amount of E·Mg^{2+}-[1-^{3}H]geranyl-PP which is trapped and is expressed as a mole fraction of E_{tot}, N is the number of turnovers at $t = \infty$, and f_t is the fraction of [1-^{14}C,5-^{3}H]farnesyl-PP produced at time t. T, the mole fraction of E·Mg^{2+}-[1-^{3}H]geranyl-PP trapped, was calculated from P according to eq 14. ^{3}H/^{14}C ratios were obtained for [1-^{14}C,5-^{3}H]farnesol purified by TLC, while values for f_t were determined by dividing the acid-labile counts at time t by those

$$\frac{DPM_{^3H}{}^t}{DPM_{^{14}C}{}^t} = \left(\frac{S_1P}{S_3N}\right)\frac{1}{f_t} + \frac{S_2}{S_3} \qquad (13)$$

$$T = P\left(\frac{E_{tot}}{E\cdot Mg^{2+}\text{-geranyl-PP}}\right) \qquad (14)$$

Table II: Trapping E·Mg^{2+}-[1-^{3}H]Geranyl-PP with Intermediate Concentrations of Isopentenyl-PP

	before chase				after chase					
run	enzyme (μM)	Mg^{2+}-[1-^{3}H]-geranyl-PP (μM)	S_1 (μCi/μmol)	E·Mg^{2+}-[1-^{3}H]-geranyl-PP[a] (μM)	Mg^{2+}-[1-^{3}H]-geranyl-PP (mM)	S_2 (μCi/μmol)	Mg^{2+}-[1-^{14}C]-isopentenyl-PP (μM)	S_3 (μCi/μmol)	slope	T
1[b]	0.27	2.2	69	0.24	1.08	0.09	495	4.7	5.8×10^{-3}	1.0
2[c]	0.26	2.2	69	0.23	1.08	0.09	495	4.7	6.6×10^{-3}	1.0
3[c]	0.21	2.2	69	0.19	1.08	0.09	22	10.4	6.6×10^{-2}	1.0
4[c]	0.21	2.2	69	0.19	1.08	0.09	22	10.4	5.9×10^{-2}	1.0
5[c]	1.04	3.0	69	0.95	1.08	0.12	7.3	20	0.22	1.0
6[c]	0.81	3.0	69	0.74	1.08	0.12	5.0	20	0.44	1.0

[a] On the basis of $K_{diss} = 0.28$ μM (Reed & Rilling, 1976). [b] 10 °C. [c] 4 °C.

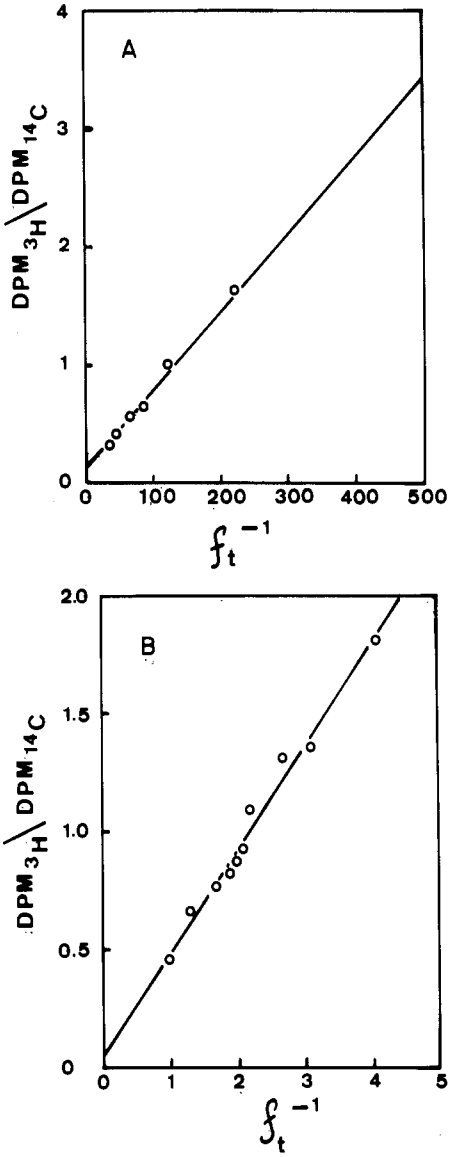

FIGURE 2: Plots of $DPM_{^3H}/DPM_{^{14}C}$ vs. f_t^{-1} for run 2 (A) and run 6 (B). Conditions are listed in Table II.

obtained at infinite time. The conditions for individual experiments are summarized in Table II, and plots of typical runs are presented in Figure 2. As before, individual points are the average of duplicate determinations, and slopes and intercepts were determined by a least-squares analysis. T equals unity, within experimental error, for all six runs, indicating that E·Mg^{2+}-[1-^{3}H]geranyl-PP is completely trapped when the concentration of Mg^{2+}-isopentenyl-PP is above 5 μM.

As illustrated by eq 13, the percent trap can be extracted from the slope of plots of $DPM_{^3H}/DPM_{^{14}C}$ vs. the inverse of mole fraction of farnesyl-PP which has been formed. However, in cases where the dissociation constant for the enzyme-substrate complex is small and the complex is efficiently trapped, the experiments become operationally difficult. Since the plots shown in Figure 2 are reciprocal in f_t, the $^3H/^{14}C$ values change most rapidly for low values of f_t. But at low conversions, with 5 μM or less of Mg^{2+}-isopentenyl-PP in the trap solution, not enough radioactivity is obtained in the product for an accurate determination of $^3H/^{14}C$ without using large reaction volumes. We took advantage of the fact that the 1′–4 condensation catalyzed by farnesyl-PP synthetase is irreversible to construct another set of experiments more suited to trapping E·Mg^{2+}-[1-^{3}H]geranyl-PP with low concentrations of Mg^{2+}-[1-^{14}C]isopentenyl-PP. Since Mg^{2+}-[1-^{14}C]isopentenyl-PP is the limiting reagent after the chase is added, the value of $DPM_{^3H}/DPM_{^{14}C}$ at $t = \infty$ depends on the extent to which Mg^{2+}-[1-^{3}H]geranyl-PP is trapped in the first turnover (see Theory). If the specific activities of the substrates are adjusted so that $S_2 \ll S_3$, at infinite reaction times, $f_t = 1$ and eq 13 becomes

$$(DPM_{^3H}/DPM_{^{14}C})_\infty = S_1P/S_3N \qquad (15)$$

At $t = \infty$, sufficient amounts of [1-^{14}C,5-^{3}H]farnesol can be isolated to measure the $^3H/^{14}C$ ratio accurately, even when the concentration of Mg^{2+}-[1-^{14}C]isopentenyl-PP in the chase is 1 μM or less.

This technique was applied to farnesyl-PP synthetase by equilibration of the enzyme with Mg^{2+}-[1-^{3}H]geranyl-PP at 4 °C followed by a chase containing Mg^{2+}-[1-^{14}C]isopentenyl-PP and unlabeled Mg^{2+}-geranyl-PP. The resulting solution was held at 4 °C for a short period of time, and the incubation was continued at 37 °C to allow the reaction to proceed to completion. Samples were removed and worked up as outlined in Scheme IV. The results are summarized in Table III. At concentrations for Mg^{2+}-isopentenyl-PP of 5 μM and above, 100% of E·Mg^{2+}-[1-^{3}H]geranyl-PP was trapped, confirming the results obtained from the time-dependent $^3H/^{14}C$ isotope ratio experiments. However, when the concentration of Mg^{2+}-isopentenyl-PP in the trap solution dropped to 3.2 μM or below, dissociation of E·Mg^{2+}-geranyl-PP prior to addition of Mg^{2+}-[1-^{14}C]isopentenyl-PP and catalysis was measurable. The effect of varying Mg^{2+}-isopentenyl-PP concentration in the chase solution of runs 3–5 is shown in Figure 3. A plot of T^{-1} vs. [Mg^{2+}-[1-^{14}C]isopentenyl-PP]$^{-1}$ gives a value of 1.4 μM for the concentration required for half-maximal trapping of the binary E·Mg^{2+}-geranyl-PP complex ($K_{1/2}$) and a limiting value of 115% for the efficiency of trapping of the binary complex (Rose et al., 1974; Cleland, 1975). Finally, it should be noted that this procedure completely eliminates the need for a quench step with enzymes that catalyze irreversible reactions.

Table III: Trapping Geranyl-PP at Low Concentrations of Isopentenyl-PP[a]

	before chase				after chase				
run	enzyme (μM)	Mg^{2+}-[1-^{3}H]-geranyl-PP (μM)	S_1 (μCi/μmol)	E·Mg^{2+}-[1-^{3}H]-geranyl-PP[b] (μM)	Mg^{2+}-[1-^{3}H]-geranyl-PP (mM)	S_2 (μCi/μmol)	Mg^{2+}-[1-^{14}C]-isopentenyl-PP (μM)	S_3 (μCi/μmol)	T
1	0.58	7.4	69	0.50	1.08	0.28	9.6	20	1.0
2	0.43	7.4	69	0.37	1.08	0.28	6.0	20	1.0
3	0.43	7.4	69	0.37	1.08	0.28	3.2	20	0.75
4	0.43	7.4	69	0.37	1.08	0.28	2.0	20	0.60
5	0.43	7.4	69	0.37	1.08	0.28	1.1	20	0.44

[a] 4 °C. [b] On the basis of the K_{diss} = 0.28 μM (Reed & Rilling, 1976).

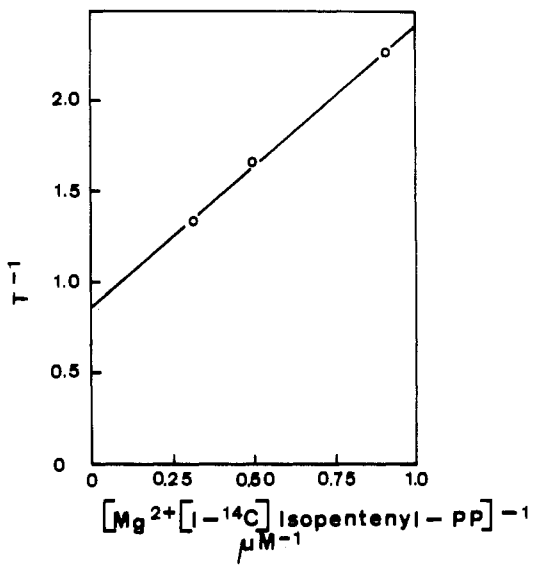

FIGURE 3: A plot of $(Mg^{2+}$-[1-^{14}C]isopentenyl-PP$)^{-1}$ in the chase vs. T^{-1} for trapping of E·Mg^{2+}-[1-^{3}H]geranyl-PP. Conditions are presented in Table III.

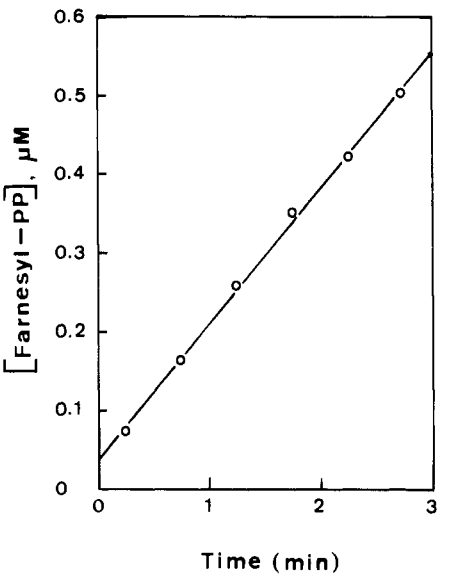

FIGURE 4: Rate of synthesis of [1-^{14}C]farnesyl-PP between 15 s and 3 min. Initial concentrations were 0.03 μM farnesyl-PP synthetase, 4.5 μM [1-^{14}C]isopentenyl-PP (56 μCi/μmol), and 16 μM geranyl-PP in 2.0 mL of 10 mM Pipes buffer, pH 7.0, 10 mM β-mercaptoethanol, and 1 mM magnesium chloride at 4 °C.

The absence of any trapping of E·Mg^{2+}-isopentenyl-PP does not completely rule out the possibility of a random sequential mechanism (Wilkinson & Rose, 1979) although the (2×10^3)-fold difference between the value of $K_{1/2}$ for half-maximal trapping of E·Mg^{2+}-geranyl-PP by Mg^{2+}-isopentenyl-PP and the maximum concentration of Mg^{2+}-geranyl-PP used in attempts to trap E·Mg^{2+}-isopentenyl-PP indicates that the reaction is ordered for all practical purposes.

Observation of a Burst Phase. When the rate of synthesis of farnesyl-PP was measured for incubations containing high concentrations of farnesyl-PP synthetase, a linear plot with a nonzero intercept was obtained, as shown in Figure 4. The extrapolated value for synthesis of farnesyl-PP at zero time is 0.036 ± 0.006 μM and within experimental error of the concentration of catalytic sites in solution. A distinct burst phase (see Figure 5) was observed when the rate of formation of farnesyl-PP was measured between 0.24 and 10.04 s by using a multimixing machine for rapid quenching. An average steady-state rate of 0.10 s^{-1} was extracted from the linear portion of the curve. The rate constant for the burst phase was evaluated by subtraction of individual time points from the extrapolated steady-state values (Shafer et al., 1972). The semilog plot of the resulting difference, shown in the inset in Figure 5, is characterized by a single exponential with a rate constant of 4.8 s^{-1}. Since farnesyl-PP is the only radiolabeled acid-labile material in the incubation mixture, the burst of radioactivity is a direct measure of the total concentration of farnesyl-PP, both free and bound. Thus, the faster rate, k = 4.7 s^{-1}, represents formation of Mg^{2+}-farnesyl-PP on the surface of the enzyme, and the slower rate, k = 0.1 s^{-1}, represents a postcatalytic event such as isomerization of E·Mg^{2+}-farnesyl-PP·Mg^{2+}-PP_i or dissociation of the E·product complex.

Determination of the Michaelis Constant for Isopentenyl-PP at 4 °C. The Michaelis constant for isopentenyl-PP was determined at 4 °C by a nonlinear least-squares fit of time-course measurements to the integrated form of the Michaelis–Menten equation for the 1′–4 condensation reaction (Laskovics et al., 1979). The value at 4 °C, $K_M^{isopentenyl\text{-}PP}$ = 0.1 μM, is, within experimental error, equal to that obtained at 37 °C.

Evaluation of Rate Constants in the 1′–4 Condensation Reaction. When the ordered sequential mechanism for the 1′–4 condensation reaction shown in Scheme V is assumed, the overall process can be dissected into six individual steps whose kinetic constants can be evaluated. Rose and his coworkers (Rose et al., 1974) were the first to use isotope partitioning to evaluate the rate of dissociation (k_2) of the binary enzyme·substrate complex for a bisubstrate reaction and derived an expression for k_2 by integration of the differential equations for the system. Shortly afterward, Cleland reported a simpler derivation of Rose's equation using partition analysis (Cleland, 1975). Following Cleland's approach, the rate of dissociation of enzyme·Mg^{2+}-geranyl-PP (k_2) equals the net rate constant for formation of farnesyl pyrophosphate in a single turnover experiment at the concentration of Mg^{2+}-isopentenyl-PP ($K_{1/2}$) required to trap one-half of the binary complex.

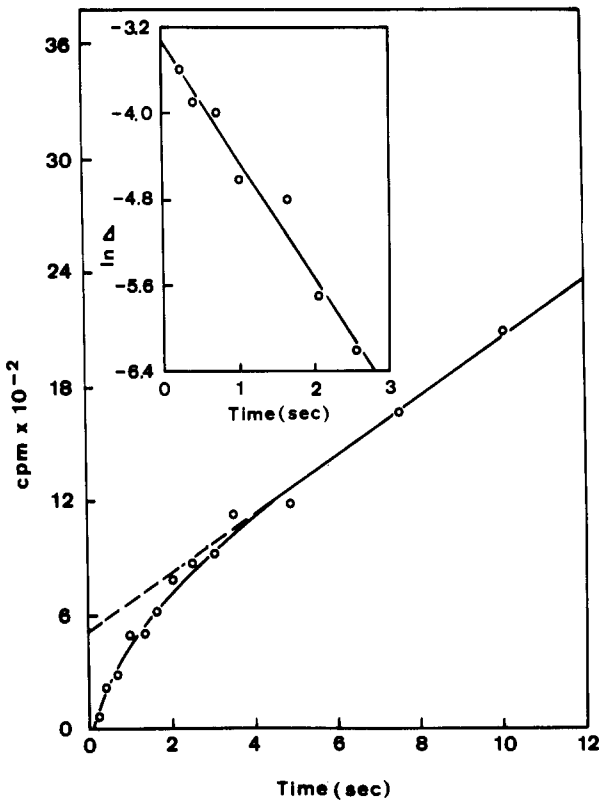

FIGURE 5: Rate of synthesis of [1-^{14}C]farnesyl-PP between 0.24 and 10 s. Initial concentrations after mixing were 0.05 μM farnesyl-PP synthetase, 5 μM [1-^{14}C]isopentenyl-PP (56 μCi/μmol), and 18 μM geranyl-PP in 10 mM Pipes buffer, pH 7.0, 10 mM β-mercaptoethanol, 1 mM magnesium chloride, and 0.1% BSA at 4 °C. (Inset) Semilog plot of the difference, Δ, between the concentration of [1-^{14}C]-farnesyl-PP and values extrapolated from the linear portion of the curve as a function of time.

$$k_2 = \frac{k_3 k_5 K_{1/2}}{k_4 + k_5} \tag{16}$$

Accounting for the observations that catalysis is irreversible and a postcatalytic step is rate limiting, the Michaelis constant for isopentenyl-PP derived by using the King–Altman procedure (Segal, 1975) is

$$K_M^{\text{isopentenyl-PP}} = \frac{k_6(k_4 + k_5)}{k_3(k_5 + k_6)} \tag{17}$$

and upon substitution, the expression for k_2 becomes

$$k_2 = \frac{k_5 k_6 K_{1/2}}{(k_5 + k_6) K_M^{\text{isopentenyl-PP}}} \tag{18}$$

Since the steady-state rate constant, k_s (or V_{max}/E_{tot}), is

$$k_s = \frac{V_{max}}{E_{tot}} = \frac{k_5 k_6}{k_5 + k_6} \tag{19}$$

eq 18 becomes

$$k_2 = \frac{V_{max} K_{1/2}}{E_{tot} K_M^{\text{isopentenyl-PP}}} \tag{20}$$

Values of $V_{max}/E_{tot} = 0.1\ s^{-1}$, $K_{1/2} = 1.4\ \mu M$, and $K_M^{\text{isopentenyl-PP}} = 0.10\ \mu M$ were obtained from isotope partitioning and time–course measurements. The rate constant for the transient burst (k_t) seen in the irreversible 1′–4 condensation is given by the sum of the condensation (k_5) and postcatalytic (k_6) rate constants (see eq 21), while the steady-state rate constant, k_s,

$$k_t = k_5 + k_6 \tag{21}$$

Scheme V: Ordered Sequential Mechanism for Farnesyl-PP Synthetase

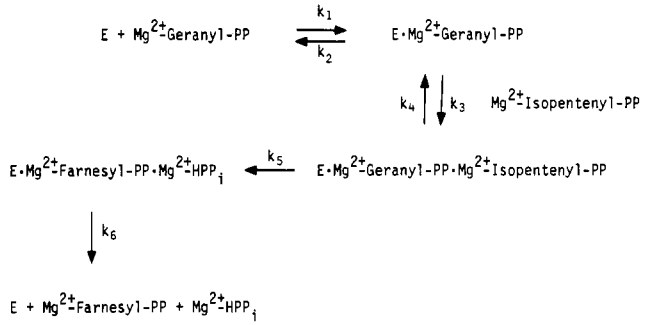

is related to k_5 and k_6 as shown in eq 19. When the values $k_s = 0.10\ s^{-1}$ and $k_t = 4.8\ s^{-1}$ obtained from the rapid quench data are used, 19 and 21 give $k_5 = 4.7\ s^{-1}$ and $k_6 = 0.10\ s^{-1}$. The rate constant for dissociation of E·Mg^{2+}-geranyl-PP (k_2) determined from eq 18 is $1.4\ s^{-1}$. Furthermore, King & Rilling (1977) measured a dissociation constant of 0.28 μM for E·Mg^{2+}-geranyl-PP at 4 °C. Thus, the rate constant for addition of the allylic substrate (k_1) calculated from eq 22 is 4.9×10^6

$$K_{diss}^{\text{Mg}^{2+}\text{-geranyl-PP}} = k_2/k_1 \tag{22}$$

$M^{-1}\ s^{-1}$. Values for k_3 and k_4 can be obtained from the simultaneous solution of eq 17 and 23.

$$K_{diss}^{\text{Mg}^{2+}\text{-isopentenyl-PP}} = k_4/k_3 \tag{23}$$

The dissociation constant ($K_{diss}^{\text{Mg}^{2+}\text{-isopentenyl-PP}}$) for release of the homoallylic substrate from E·Mg^{2+}-geranyl-PP·Mg^{2+}-isopentenyl-PP cannot be evaluated directly. Reed & Rilling (1976) did discover, however, that the enzyme forms a ternary complex with two molecules of Mg^{2+}-isopentenyl-PP per active site and measured a dissociation constant of 2.5 μM. Three lines of evidence suggest that this value is close to the dissociation constant when the allylic site is occupied by an allylic substrate rather than by Mg^{2+}-isopentenyl-PP. First, the dissociation constant is only slightly larger than 2.5 μM when Mg^{2+}-2,3-dihydrogeranyl-PP, a potent competitive inhibitor of Mg^{2+}-geranyl-PP, occupies the allylic region of the active site (Reed & Rilling, 1976). Second, the dissociation constant for isopentenyl-PP in the metal-free ternary complex with geranyl pyrophosphate is only slightly larger than that for E·(Mg^{2+}-isopentenyl-PP)$_2$ (King & Rilling, 1977). Finally, space-filling models indicate that the hydrocarbon moiety in isopentenyl-PP can adopt conformations whose topologies are very similar to those of the natural C_5 allylic substrate dimethylallyl-PP, thereby mimicking the substrate normally bound in the allylic region of the active site. Using the value of 2.5 μM in eq 23 and solving eq 17 and 23 simultaneously give $k_3 = 2 \times 10^6\ M^{-1}\ s^{-1}$ and $k_4 = 5\ s^{-1}$. The kinetic constants are summarized in Table IV.

Evaluation of Dissociation Constants for Enzyme·(Mg^{2+}-PP$_i$)$_2$ and Enzyme·Mg^{2+}-PP$_i$. Recently, Rilling and Saito published a Scatchard plot for avian liver farnesyl-PP synthetase and PP$_i$ in the presence of Mg^{2+} (Saito & Rilling, 1979) which showed marked curvature. We fit their data to an interacting site, noninteracting subunit model (Hammes & Wu, 1974) using a nonlinear least-squares routine developed by Powell & Macdonald (1972). Each concentration was corrected for the amount of Mg^{2+}-PP$_i$ present in solution (approximately 10% of the total PP$_i$) since previous kinetic experiments indicated that the monomagnesium salt is the species bound (Laskovics et al., 1979). The correction results in a severalfold reduction relative to values based on total PP$_i$. The original data and the calculated curve are presented in

Table IV: Values for the Individual Kinetic Constants of the 1′-4 Condensation Reaction Catalyzed by Avian Liver Farnesyl-PP Synthetase[a,b]

constant	value
k_1	4.9×10^6 M^{-1} s^{-1}
k_2	1.4 s^{-1}
k_3	2×10^6 M^{-1} s^{-1}
k_4	5 s^{-1}
k_5	4.7 s^{-1}
k_6	0.1 s^{-1}

[a] Defined in Scheme IV. [b] 4 °C.

Figure 6. Dissociation constants for $E\cdot(Mg^{2+}\text{-}PP_i)_2$ and $E\cdot Mg^{2+}\text{-}PP_i$ are estimated to be 0.38 μM and 7.7 μM, respectively.

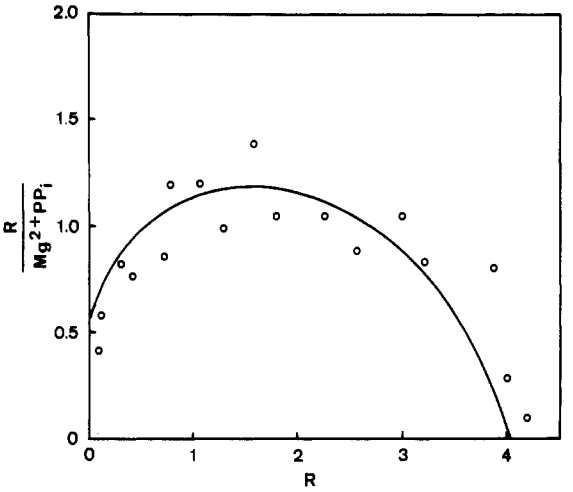

FIGURE 6: Binding of Mg^{2+}-$^{32}PP_i$ at 4 °C, where R is the ligand bound per mole of enzyme and Mg^{2+}-PP_i is the concentration of free monometal salt. The enzyme concentration was 4.8 μM. The curve is a nonlinear least-squares fit based on an interacting site, noninteracting subunit model. Data are from Saito & Rilling (1979).

Discussion

The active site of farnesyl-PP synthetase catalyzes two sequential 1′–4 condensation reactions. The first adds the hydrocarbon moiety of dimethylallyl-PP to isopentenyl-PP, and the second adds the hydrocarbon moiety of geranyl-PP to isopentenyl-PP. During the synthesis of farnesyl-PP from dimethylallyl-PP, geranyl-PP is released from the surface of the enzyme before addition of a second molecule of isopentenyl-PP (Poulter & Rilling, 1978). Binding studies indicate that the active site has two distinct binding regions. One, denoted as the allylic region, binds the allylic substrates, the allylic product farnesyl-PP, and isopentenyl-PP, while the other is specific for isopentenyl-PP. In view of the topological similarities among substrates and products, especially that between the hydrocarbon residues of isopentenyl-PP and dimethylallyl-PP, the specificity exhibited by the homoallylic region of the active site is both remarkable and important for maintaining optimal catalytic efficiency.

Previous studies on the mechanism of substrate binding have not been conclusive. Several lines of evidence from this and other laboratories, including kinetic studies (Laskovics et al., 1979; Holloway & Popjak, 1967; Popjak et al., 1969), an attempt to detect a partial reaction with geranyl-PP (Poulter & Rilling, 1978), and an attempt at affinity labeling (Poulter et al., 1979), all indicate that farnesyl-PP synthetase operates by a sequential mechanism. The choice between a random and an ordered addition of the substrates cannot, however, be made on the basis of initial velocity patterns because isopentenyl-PP and, by implication, analogues of isopentenyl-PP do not bind regiospecifically to the homoallylic region of the active site (Laskovics et al., 1979).

At this point, we turned to isotope trapping techniques (Rose et al., 1974; Caperelli et al., 1978; Raushel & Villafranca, 1979) to make the distinction. Mg^{2+}-geranyl-PP forms a binary complex with farnesyl-PP synthetase that is efficiently trapped by Mg^{2+}-isopentenyl-PP, with $K_{1/2}$ = 1.4 μM. Interpretation of partitioning experiments with $E\cdot Mg^{2+}$-isopentenyl-PP is not as straightforward. Kinetic and dialysis measurements indicate that Mg^{2+}-isopentenyl-PP interacts with both the homoallylic and the allylic regions of the active site. Under such conditions, four forms of the enzyme, (1) free enzyme, (2) $E\cdot Mg^{2+}$-[1-^{14}C]isopentenyl-PP with substrate in the homoallylic region, (3) $E\cdot Mg^{2+}$-[1-^{14}C]isopentenyl-PP with substrate in the allylic region, and (4) $E\cdot(Mg^{2+}$-[1-^{14}C]isopentenyl-PP$)_2$, are possible. Of the four, only the binary complex with Mg^{2+}-isopentenyl-PP in the homoallylic region can combine directly with Mg^{2+}-geranyl-PP to generate a catalytically competent ternary complex. The linear Scatchard plot obtained by Reed & Rilling (1976) can be interpreted most directly in terms of two-step process where Mg^{2+}-isopentenyl-PP combines with farnesyl-PP synthetase to give a single binary complex followed by addition of a second molecule of the substrate, with dissociation constants of 2.5 μM for both the binary and ternary complexes. There is some scatter in their binding data, and one cannot rule out a small equilibrium population of a second binary complex. However, the inability to detect any trapping of an $E\cdot Mg^{2+}$-isopentenyl-PP species with 2 mM Mg^{2+}-geranyl-PP, while $E\cdot Mg^{2+}$-geranyl-PP is completely trapped by 5 μM Mg^{2+}-isopentenyl-PP indicates that for all practical purposes the reaction is ordered and Mg^{2+}-geranyl-PP adds before Mg^{2+}-isopentenyl-PP. Presumably the reaction is also ordered for addition of Mg^{2+}-dimethylallyl-PP and Mg^{2+}-isopentenyl-PP, although this point has not been proven.

The rate constants for addition of Mg^{2+}-geranyl-PP and Mg^{2+}-isopentenyl-PP, $k_1 = 4.9 \times 10^6$ M^{-1} s^{-1} and $k_3 = 2.0 \times 10^6$ M^{-1} s^{-1}, respectively, are similar and well below the value of 10^8 M^{-1} s^{-1} normally associated with a diffusion-controlled process (Hammes & Schimmel, 1970). These slower rates of addition may indicate that conformational changes in the enzyme preceed or accompany addition of the substrates.

There are also indications that conformational changes limit the rate at which farnesyl-PP dissociates. In theory, one can calculate the rate constant for addition of product to the enzyme (k_{on}) from k_6 and the appropriate dissociation constant. A slow rate ($<10^6$ M^{-1} s^{-1}) would be consistent with a conformational change in the addition process and, by the principal of microscopic reversibility, for the dissociation as well. Application of this concept to farnesyl-PP synthetase is complicated for two reasons. First, the 1′–4 condensation is irreversible, and we are thus unable to assign k_6 to a discrete postcatalytic step for calculation of k_{on}. Five processes are potentially represented by k_6: (1) dissociation of Mg^{2+}-farnesyl-PP from $E\cdot Mg^{2+}$-farnesyl-PP$\cdot Mg^{2+}$-PP_i, (2) dissociation of Mg^{2+}-PP_i from the ternary complex, (3) dissociation of Mg^{2+}-farnesyl-PP from $E\cdot Mg^{2+}$-farnesyl-PP, (4) dissociation of Mg^{2+}-PP_i from $E\cdot Mg^{2+}$-PP_i, and (5) an isomerization prior to one of the four previous events. Constants for the binary complexes with Mg^{2+}-farnesyl-PP and Mg^{2+}-PP_i are 0.28 μM (King & Rilling, 1977) and 0.4 μM, respectively. A value for dissociation of either ligand from the ternary complex is not available, but competition experiments with Mg^{2+}-farnesyl-PP

and Mg^{2+}-PP_i do not show evidence for cooperative binding of one product in the presence of the other (Saito & Rilling, 1979).

The second problem concerns the structures of E·Mg^{2+}-farnesyl-PP·Mg^{2+}-PP_i and the two binary complexes. The ternary complex generated during 1′–4 condensation has the hydrocarbon chain of Mg^{2+}-farnesyl-PP spread over the allylic and isopentenyl regions of the active site and the pyrophosphate moiety in the isopentenyl region. Mg^{2+}-PP_i is in the allylic region. This structure is not the major form of the enzyme when farnesyl-PP synthetase is mixed with its products. The patterns of double-reciprocal plots (Laskovics et al., 1979) clearly indicate that Mg^{2+}-farnesyl-PP prefers to add with its pyrophosphate residue in the allylic region as if it were an allylic substrate. Under forcing conditions, 1′–4 condensation between farnesyl-PP and isopentenyl-PP is observed (Poulter & Rilling, 1978). Competition experiments indicate that Mg^{2+}-farnesyl-PP prefers to remain in the allylic region in the presence of a variety of molecules, including Mg^{2+}-PP_i (Reed & Rilling, 1976; King & Rilling, 1977; Saito & Rilling, 1979). Thus, the dissociation constant needed for the calculation of k_{on} should be substantially larger than the values reported from equilibrium measurements. On the basis of $K_{diss}^{k_5} \geq 0.1$ μM, an extremely conservative estimate of the *maximum* value for k_{on} is 10^6 M^{-1} s^{-1}. Rate constants smaller than 10^6 M^{-1} s^{-1} are clearly beyond the diffusion-controlled limit, and a conformational relaxation is indicated for the slow step of the 1′–4 condensation.

Since farnesyl-PP synthetase catalyzes sequential C_5 homologations and the product of the first reaction (dimethylallyl-PP to geranyl-PP) is the substrate for the second (geranyl-PP to farnesyl-PP), a conformational process which restricts binding of allylic substrates (and expecially geranyl-PP) to the allylic region of the active site would be productive. It will be interesting to see if this is a general phenomenom for 1′–4 polyprenyl synthetases, especially for those enzymes involved in biosynthesis of ubiquinones and dolichols. Finally, if k_6 is compared with k_5, farnesyl-PP is synthesized 47 times faster than the rate-limiting postcatalytic step during prenyl transfer. Thus, farnesyl-PP synthetase represents another case of an enzyme which has evolved to the point where further improvements in the catalytic step are of no value (Knowles & Albery, 1977).

References

Bernard, G. F., Langton, B., & Popjak, G. (1978) *Biochem. Biophys. Res. Commun. 85*, 1097.

Caperelli, C. A., Frey, W. A., & Benkovic, S. J. (1978) *Biochemistry 17*, 1699.

Cleland, W. W. (1975) *Biochemistry 14*, 3220.

Cornforth, R. H., & Popjak, G. (1969) *Methods Enzymol. 15*, 359.

Cramer, W. D., & Weiman, G. (1960) *Chem. Ind. (London)*, 46.

Donninger, C., & Popjak, G. (1967) *Biochem. J. 105*, 545.

Eberhardt, N. L., & Rilling, H. C. (1975) *J. Biol. Chem. 250*, 863.

Hammes, G. G., & Schimmel, P. R. (1970) *Enzymes, 3rd Ed.*, 67.

Hammes, G. G., & Wu, C. W. (1974) *Annu. Rev. Biophys. Bioeng. 3*, 1.

Holloway, P. W., & Popjak, G. (1967) *Biochem. J. 104*, 57.

King, H. L., & Rilling, H. C. (1977) *Biochemistry 16*, 3815.

Knowles, J. R., & Albery, W. J. (1977) *Acc. Chem. Res. 10*, 105.

Laskovics, F. M., Krafcik, J. M., & Poulter, C. D. (1979) *J. Biol. Chem. 254*, 9458.

Popjak, G., Holloway, P. W., Bond, R. P. M., & Robuts, M. (1969) *Biochem. J. 111*, 333.

Poulter, C. D., & Rilling, H. C. (1976) *Biochemistry 15*, 1079.

Poulter, C. D., & Rilling, H. C. (1978) *Acc. Chem. Res. 11*, 307.

Poulter, C. D., Marsh, L. L., Hughes, J. M., Argyle, J. C., Satterwhite, D. M., Goodfellow, R. J., & Moesinger, S. G. (1977) *J. Am. Chem. Soc. 99*, 3816.

Poulter, C. D., Mash, E. A., Argyle, J. C., Muscio, O. J., & Rilling, H. C. (1979) *J. Am. Chem. Soc. 101*, 6761.

Powell, D. R., & Macdonald, J. R. (1972) *Comput. J. 15*, 148.

Raushel, F. M., & Villafranca, J. J. (1979) *Biochemistry 18*, 3424.

Reed, B. C., & Rilling, H. C. (1975) *Biochemistry 14*, 50.

Reed, B. C., & Rilling, H. C. (1976) *Biochemistry 15*, 3739.

Richards, O. C., & Boyers P. D. (1965) *J. Mol. Biol. 11*, 327.

Rose, I. A., O'Connell, E. L., Litwin, S., & Bar Tana, J. (1974) *J. Biol. Chem. 249*, 5163.

Saito, A., & Rilling, H. C. (1979) *J. Biol. Chem. 254*, 8511.

Segel, I. H. (1975) *Enzyme Kinetics*, pp 560–593, 646, Wiley, New York.

Shafer, J. A., Chiancone, E., Yielding, K. L., & Antonini, E. (1972) *Eur. J. Biochem. 28*, 528.

Wilkinson, K. D., & Rose, I. A. (1979) *J. Biol. Chem. 254*, 12567.

Yeh, L. S., & Rilling, H. C. (1977) *Arch. Biochem. Biophys. 183*, 718.